Cancer Cell International

RESEARCH

Open Access

Expression of stearoyl coenzyme a desaturase in neuronal cells facilitates pancreatic cancer progression

Xue Zhang[1], Ling-Xiao Zhao[2], Si-Qi Cheng[3] and Ye-Fu Liu[4*]

Abstract

Background Pancreatic adenocarcinoma (PDAC) is the most fatal malignant tumor that focuses on men and the elderly (40–85 years) and is aggressive. Its surgical resection rate is only 10-44%, and the rate of local recurrence in the retroperitoneum 1 year after surgery is as high as about 60%. The main reason for local recurrence in the majority of patients is that PDAC is perineural invasion (PNI) and the cancer cells infiltrate and grow along the peripancreatic nerve bundles. The identification of biomarkers associated with the diagnosis of PDAC may help to improve the current difficulty in early diagnosis of pancreatic cancer and guide clinical treatment. We constructed a co-culture model system of Schwann and PDCA cells to determined that Stearoyl Coenzyme A Desaturase (SCD) is a key gene driving the progress of PDAC.

Methods Single-cell data files for PDAC were analyzed to compare cellular composition and subpopulation-specific gene expression between control ($n=4$) and pancreatic cancer ($n=6$). Among 36,277 cells, we obtained a total of 16 subpopulations, including a Neurons subpopulation, by UMAP analysis. Further screening by Mendelian randomization analysis yielded three pairs of key genes corresponding to eQTL-positive outcome causally, the corresponding genes were, in order: the three genes COL18A1, RASSF4, and SCD. Among them, SCD was significantly positively correlated with with the malignant progression of pancreatic cancer, and enriched in signaling pathways such as MTORC1_SIGNALING and P53-PATHWAY. In this study, We further applied CRISPR-Cas9 technology to knock out SCD expression in Schwann cells under co culture system to detect the growth status of PDAC cells.

Results Three genes (COL18A1, RASSF4, SCD) showed significant correlation with PDAC. The identified SCD genes were positively correlated with the development of PDAC. We further demonstrated through experiments that SCD is overexpressed in PDAC tissues, and knocking down SCD in neuronal cells reduces the PDAC cells growth rate and migration ability.

Conclusion In this article, we demonstrated that the upregulation of SCD expression level in neuronal cells is related to the PDAC, and SCD may be a promising candidate for PDAC therapy.

Keywords Pancreatic ductal adenocarcinoma, Mendelian randomization, Peripheral nerves

*Correspondence:
Ye-Fu Liu
97902153@cmu.edu.cn

Full list of author information is available at the end of the article

Introduction

PDAC is a malignant tumor originating from the epithelium and follicular cells of the pancreatic ducts [1]. Several studies have identified elderly age, tobacco use and a long-history chronic pancreatitis as clear risk factors, both diabetes and obesity also appear to increase risk of cancer [1–3]. Increased risk in relatives of patients with PDAC has been documented, with an estimated 10% of PDAC cases having a genetic susceptibility based on familial clustering [4, 5]. Accordingly, germline mutations were associated with familial PDAC, including mutations targeting the oncogenes INK4A, BRCA2, and LKB1, the cationic trypsinogen gene PRSS1, and the DNA mismatch repair gene MLH1 [6, 7]. BRCA1 mutations appear to increase susceptibility to PDAC, although the associated risk is lower than BRCA2 [8]. Cancer Data 2022 statistics show that PDAC mortality ranks as the fourth leading cause of tumor-related death [9]. Its mortality to incidence M/I ratio (MIR) is about 0.94, which is the first among all common tumor types, reflecting its extremely high degree of malignancy and poor prognosis, and posing a more serious challenge to basic translational and clinical research in PDAC [10]. Therefore, the identification of PDAC predisposing factors and biomarkers affecting the progression of PDAC is necessary, in order to select the best treatments for patients with PDAC, thus providing the best hope for a cure or prolonged life expectancy.

Prominent perineural alterations such as an increase in the size of neural hypertrophy and some intrapancreatic nerves, neural density, and neural remodeling were observed during PDAC progression [11, 12]. Growing evidence suggests active interactions between tumor and nerve cells. ADRB2-signaling pathway promotes the secretion of brain-derived neurotrophic factor (BDNF) and nerve growth factor (NGF) in PDAC, thereby increasing nerve density [13]. Schwann cell is the main cell type in peripheral nerves [14]. Remarkably, this type of cells are frequently detectable around pancreatic intraepithelial neoplasia (PanIN) lesions both in humans and mice [15]. In this study, we used Schwann cells and PDAC cells (PANC-1 and MIA PaCa-2) to establish a co-culture model to investigate the effect of SCD expression in neuronal cells on PDAC progression.

As early as 1970, Paulien Hogeweg of Utrecht University in the Netherlands coined the term "bioinformatics". She defined it as "the study of information processes in biological systems" [16]. With the development of large-scale high-throughput multi-omics technologies, such as genomics, transcriptomics, proteomics, and metabolomics, the generation of biomedical data has been greatly accumulated, further advancing the development of bioinformatics. Mendelian randomization (False Discovery Rate, FDR) is a statistical method commonly used in bioinformatics, a design which improving causal inferences from observational data by using genetic variation as a natural experiment [17, 18]. In the last decade, genome-wide association analyzes (GWAS, Genome-wide association studies) of almost all common malignancies have been completed and more than 450 genetic variants associated with increased risk have been identified, and these findings have enabled the FDR design. Recently, Mendelian randomization has been increasingly used in the identification of susceptibility genes. Bioinformatics can help to comprehensively study tumorigenesis in depth, screen possible core targets, and provide references for clinical diagnosis and disease treatment.

In this study, we analyzed a single-cell database of PDAC and further sorted the neuronal cell taxa therein, applied Mendelian randomization for genetic evolution, and screened for marker genes that can predict PDAC development. Finally, we utilized experiments to validate the association of SCD genes with the proliferative and invasive ability of pancreatic cells.

Results

Quality control

Single-cell data files based on GSE212966, we first read the expression profiles using the Seurat package, filtering cells based on total UMIs (Unique Molecular Identifiers) per cell, expressed genes, mitochondria per cell and ribosomes per cell. Among them, outliers are defined as three median absolute deviations (MAD) from the median, and cells with less than 500 captured genes will be filtered, filtering formula: (nFeature_RNA > 500 & percent.mt < = 3MAD & nFeature_RNA < = 3MAD & nCount_RNA < = 3MAD & percent.ribo < = 3MAD), where nFeature_RNA represents the number of genes, nCount_RNA represents the total number of UMIs in the cell, percent.mt represents the mitochondrial reading percentage, and percent.ribo represents the ribosome reading percentage. The DoubletFinder package was then used to filter the double cells, and a total of 36,277 cells were retained (sup Fig. 1AB). The 10 genes with the highest standard errors were displayed (sup Fig. 1C). The data were then processed by standardisation, homogenisation, PCA (Principal Component Analysis) and harmony analysis in sequence (sup Fig. 1D-F), and finally a total of 16 subgroups were obtained by UMAP (uniform manifold approximation and projection) analysis (Fig. 1A).

Cell annotation and ligand-receptor interaction analysis

This study further annotated each subtype. 11 cell categories were annotated: $CD8^+$ T cells, Fibroblasts, B cells, Epithelial cells, Macrophages, $CD4^+$ T cells, Endothelial cells, Neutrophils, Mast cells, NK cells, and Neurons (Fig. 1B). We also show the classic markers of these 11

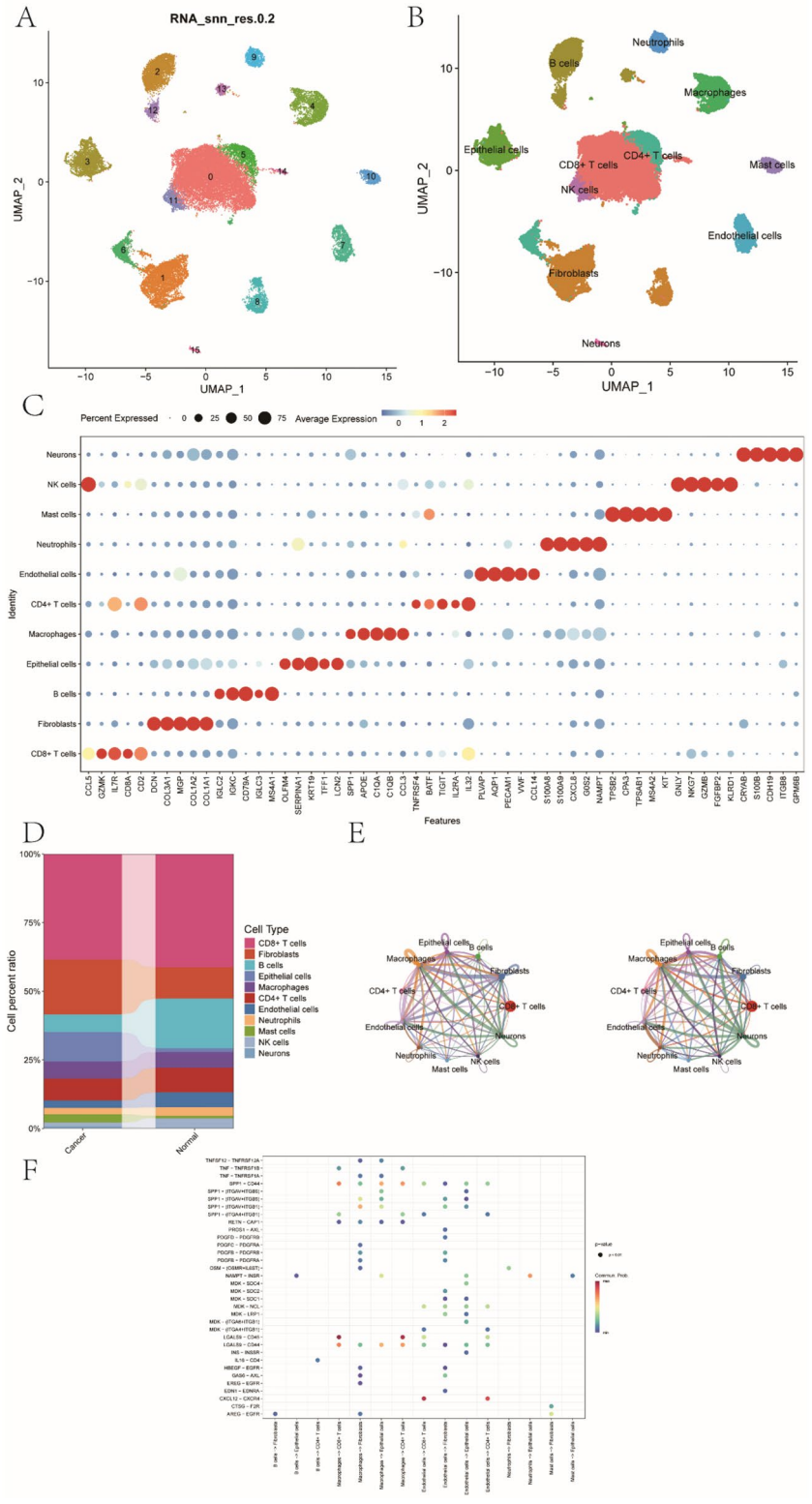

Fig. 1 (See legend on next page.)

(See figure on previous page.)

Fig. 1 Cell annotation (**A**) We used the UMAP algorithm to classify the cells into 16 clusters, based on the most important components that were available in the PCA. (**B**) Cell Annotated 16 clusters. The 16 clusters are annotated in terms of 11 different cell types, namely $CD8^+$ T cells, Fibroblasts, B cells, Epithelial cells, Macrophages, $CD4^+$ T cells, Endothelial cells, Neutrophils, Mast cells, NK cells, and Neurons. (**C**) Bubble diagram of droplet of 11 cells and their cell markers. (**D**) The difference in the proportions of these cells in both groups. (**E**) Network of cell interactions between 10 types of cells, where the width of the edges represents the probability and strength of communication between cells. Left: The size of the various coloured circles around the periphery indicates the number of cells; the larger the circle, the greater the number of cells. Cells that emit arrows express ligands, and cells to which the arrows point express receptors. The more ligand-receptor pairs, the thicker the line. Right: probability/intensity values of interactions (intensity is the probability values added together). (**F**) Cell-to-cell receptor ligand bubble diagram

cells in a bubble chart (Fig. 1C) and the histogram of cell proportions corresponding to the groups (Fig. 1D). We used the cellchat software package to analyse the ligand-receptor relationship of features in single cell expression profiles. Ultimately, we observed that there are complex associations between these cell subtypes (Fig. 1EF).

Functional analysis of GO and KEGG

Pathway analysis was also performed on the marker genes of Neurons cells. GO enrichment analysis revealed that the genes were primarily enriched in pathways such as glial cell differentiation and gliogenesis (Fig. 2A). KEGG enrichment analysis revealed that the genes were mainly clustered in adhesion molecules, cytoskeleton in muscle cells and other pathways (Fig. 2B).

Mendelian randomization analysis

In order to find out the key genes that affect PDAC, we used the marker genes obtained in the previous step and obtained the outcome ID ebi-a-GCST90018893 through the summary statistics of 476,245 samples related to PDAC (Controls: 475,049; Cases: 1,196). A total of 191 pairs of causal relationships between genes and outcomes were extracted using extract_instruments and extract_outcome_data in sequence. In addition, we demonstrated the causal relationship between three pairs of genes corresponding to positive eQTL results (Fig. 3A-C) by Mendelian randomisation analysis (IVW pval < 0.05). The corresponding genes identified are COL18A1, RASSF4 and SCD. Among them, COL18A1 (0.879; 0.790 – 0.977; $p = 0.017$); RASSF4 (0.819; 0.688 – 0.974; $p = 0.024$) may be associated with a low risk of PDAC. And SCD (1.319; 1.017 – 1.712; $p = 0.037$) may be associated with an increased risk of PDAC. To determine the reliability of the causal relationships of the three genes using the leave-one-out method, we also performed a sensitivity analysis. The results showed that the three pairs of causal relationships we selected were robust, as excluding any SNP had no apparent effect on the overall error bar (Fig. 4A-C).

GSEA pathway enrichment analysis

We then examined the specific signalling pathways which were enriched in the three key genes to explore the potential molecular mechanisms by which key genes affect PDAC progression. GSEA results revealed the pathways enriched by COL18A1 include IL-17 signaling pathway and NF-κB signaling pathway and TNF signaling pathway (Fig. 5A); pathways enriched by RASSF4 include B cell receptor signaling pathway, Chemokine signaling pathway and NF-κB signaling pathway (Fig. 5B); enriched by SCD include Glucagon signaling pathway, mRNA surveillance pathway and p53 signaling pathway (Fig. 5C). The enriched genes of related pathways are shown in sup Fig. 2. We were surprised to find that SCD correlates with the p53 pathway, which regulates cell metabolism, ferroptosis, tumor microenvironment, autophagy and so on, all of which contribute to tumor suppression [19]. This prompted us to focus on SCD.

SCD is upregulated in human pancreatic tumors

We performed immunohistochemical (IHC) analysis of SCD protein on paraformaldehyde-fixed tissue sections of pancreatic tumor samples from seven patients in order to further investigate the correlation between SCD and PDAC progression (Fig. 6AB). The presence of SCD staining was observed to be markedly prevalent within the cytoplasm of pancreatic tumor tissue, but much less in the adjacent tissue (Fig. 6C, representative results shown). A real-time fluorescence quantitative PCR (qRT-PCR) level of the patient's tissue samples showed that the transcription level of SCD in tumor tissue was up-regulated (Fig. 6D) but there was no significant difference in protein expression (Fig. 6E), which may be because SCD was only expressed in the nerve cells of PDAC.

pancreatic cancer cells (PANC-1 and MIA PaCa-2). We found that the expression level of SCD had no statistical significance on the proliferation of pancreatic cancer cells, but had a certain impact on the invasion and migration of pancreatic cancer cells (sup 3).

The depletion of SCD in Schwann cells has been demonstrated to suppress the malignant phenotypes of pancreatic tumor cells in vitro

To investigate the in vitro function of SCD in PDAC, we stably introduced Cas9 vectors containing three distinct sgRNAs that specifically target SCD or non-targeting control sgRNAs into the human Schwann cell lines (designated sgSCD-1, sgSCD-2, sgSCD-3, and sgScramble, respectively). sgSCD-1 and sgSCD-2 were selected for further experiments due to the low knockdown efficiency of sgSCD-3. The knockdown efficiency was then

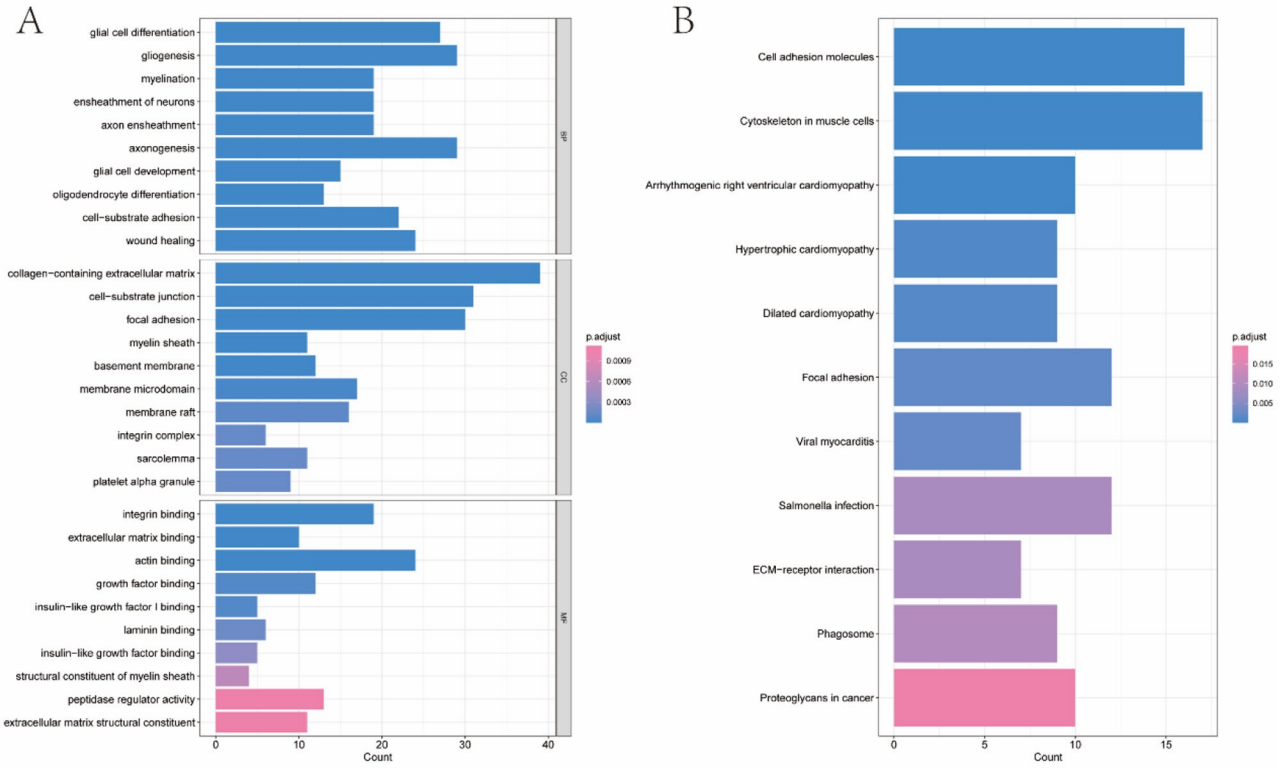

Fig. 2 Enrichment analysis. (**A**-**B**) GO-KEGG enrichment analysis based on ClusterProfiler

confirmed by IB (Fig. 7A) and qRT-PCR assay (Fig. 7B). Subsequently, a co-culture model of Schwann cells with two distinct PDAC cell lines was constructed (Fig. 7C), and a series of cell-based assays were conducted, including CCK-8 and wound healing migration assays, to elucidate the biological functions of SCD (Fig. 7D). The knockdown of SCD was observed to markedly reduce cell proliferation in sgSCD-1 and sgSCD-2 cells in comparison to their corresponding control cells. Furthermore, the wound healing migration assays demonstrated that the sgSCD-1 and sgSCD-2 cells exhibited a markedly diminished capacity to invade in comparison to the control cells (Fig. 7EF).

Discussion

Most patients with PDAC are diagnosed with locally advanced or metastatic tumors in the later stages of the disease. Despite ongoing efforts to improve PDAC treatment, patient survival remains dismal. The overall global 5-year survival rate is less than 10% [10, 20]. These facts emphasize the urgent need for a better understanding of pancreatic tumorigenesis. In this study, the analysis of neuronal cells in PDAC monocytic cells screened by Mendelian randomization yielded three pairs of genes associated with the risk of PDAC development, of which COL18A1 and RASSF4 may be associated with a low risk of PDAC. SCD, on the other hand, may be associated with high PDAC risk.

Human SCD, also called Δ9-fatty acyl-CoA desaturase, is an enzyme associated with the endoplasmic reticulum that catalyses the introduction of a double bond at the cis-Δ9 location of saturated fatty acyl-CoAs [21]. Primary substrates of SCD are palmitoyl and stearoyl CoA, which give rise to palmitoleoyl and oleoyl CoA, respectively [22]. Further studies showed that knockdown of SCD in human lung SV40-WI38 fibroblasts decreased the synthesis of MUFA and phospholipids, reduced the rate of cell proliferation and induced cell apoptosis [23]. Similarly, inhibition of SCD activity led to cancer cell death by reducing MUFA [24, 25].

Here, we report a functional analysis of the SCD gene and show that knockdown of SCD gene expression in neuronal Schwann cells significantly reduces PDAC cell proliferation and migration. SCD expression has been reported to be correlated with bad prognosis in several types of cancer [26]. Pharmacological inhibition of SCD1 as a monotherapy and in combination with chemotherapeutic agents showed promising anti-tumor potential in preclinical models [27–29]. We hypothesized that elevated SCD expression in neuronal cells may lead to elevated levels of phospholipid synthesis, and neural infiltration occurs, a process that promotes PDAC

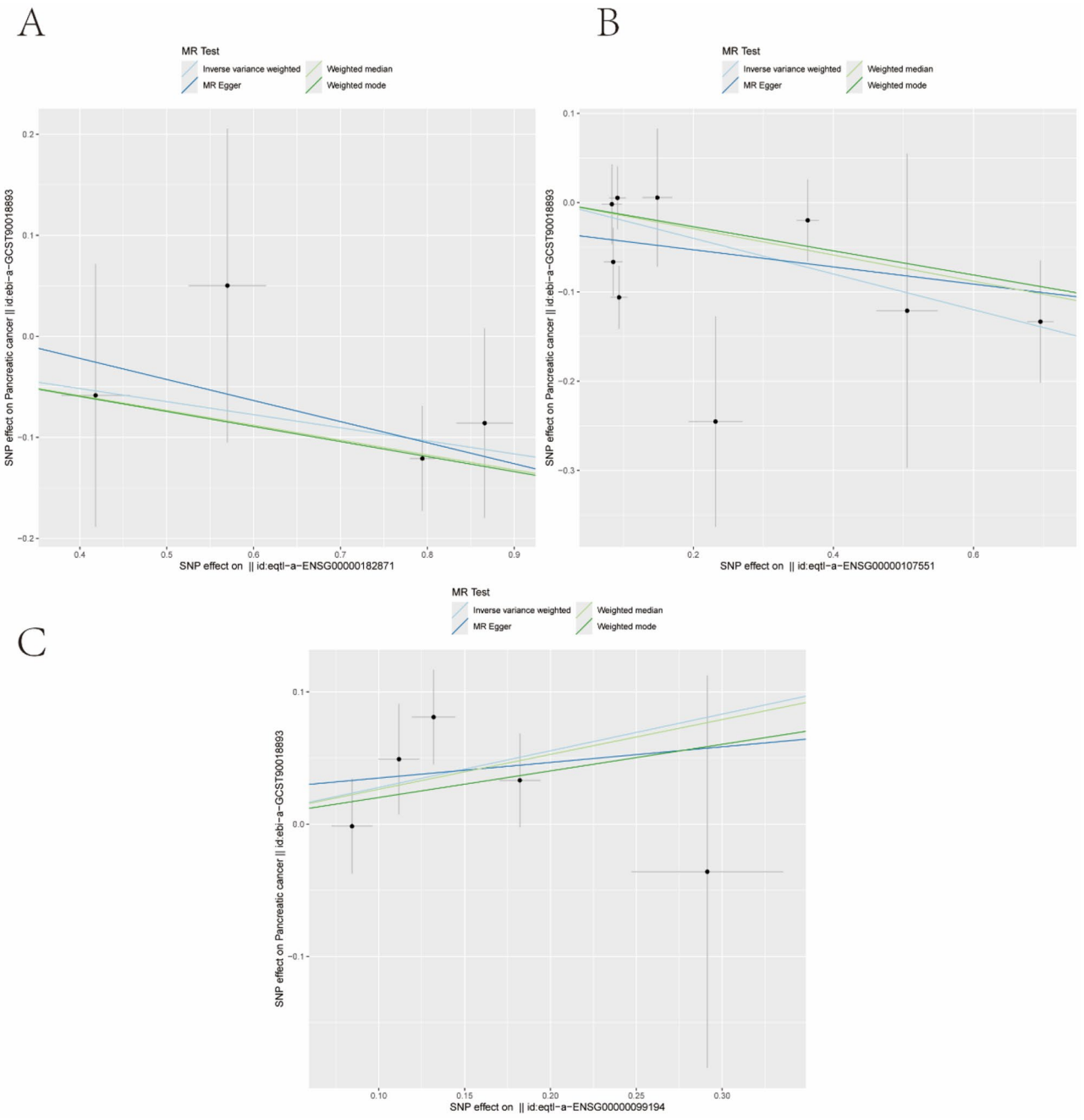

Fig. 3 Mendelian randomization analysis. (**A**-**C**) Scatterplot of MR analysis of key genes, where different colors indicate different statistical methods and the slopes of the lines indicate the causal effect of each method

progression, but evidence that SCD promotes neural infiltration in PDAC is lacking in this study.

Perineural invasion (PNI) is the process of neoplastic invasion of peripheral nerves and is considered the fifth mode of cancer metastasis. PNI has been reported in head and neck tumors, pancreatic, prostate, biliary, gastric and colorectal cancers. It is associated with poor prognosis and high local recurrence rates [30]. PNI of PDAC has become a hot research topic in academia and clinics, and its detailed mechanism has not been elucidated. In patients with PDAC, the proportion of nerve invasion can be as high as 70%~100% [31], PNI is a common post-surgical recurrence of PDAC and is an independent prognostic factor for overall survival in PDAC [32]. A study using a mouse model of pancreatic ductal adenocarcinoma found that cancer cells can produce significant structural changes to the neural microenvironment in which they invade, thus favoring their roaming

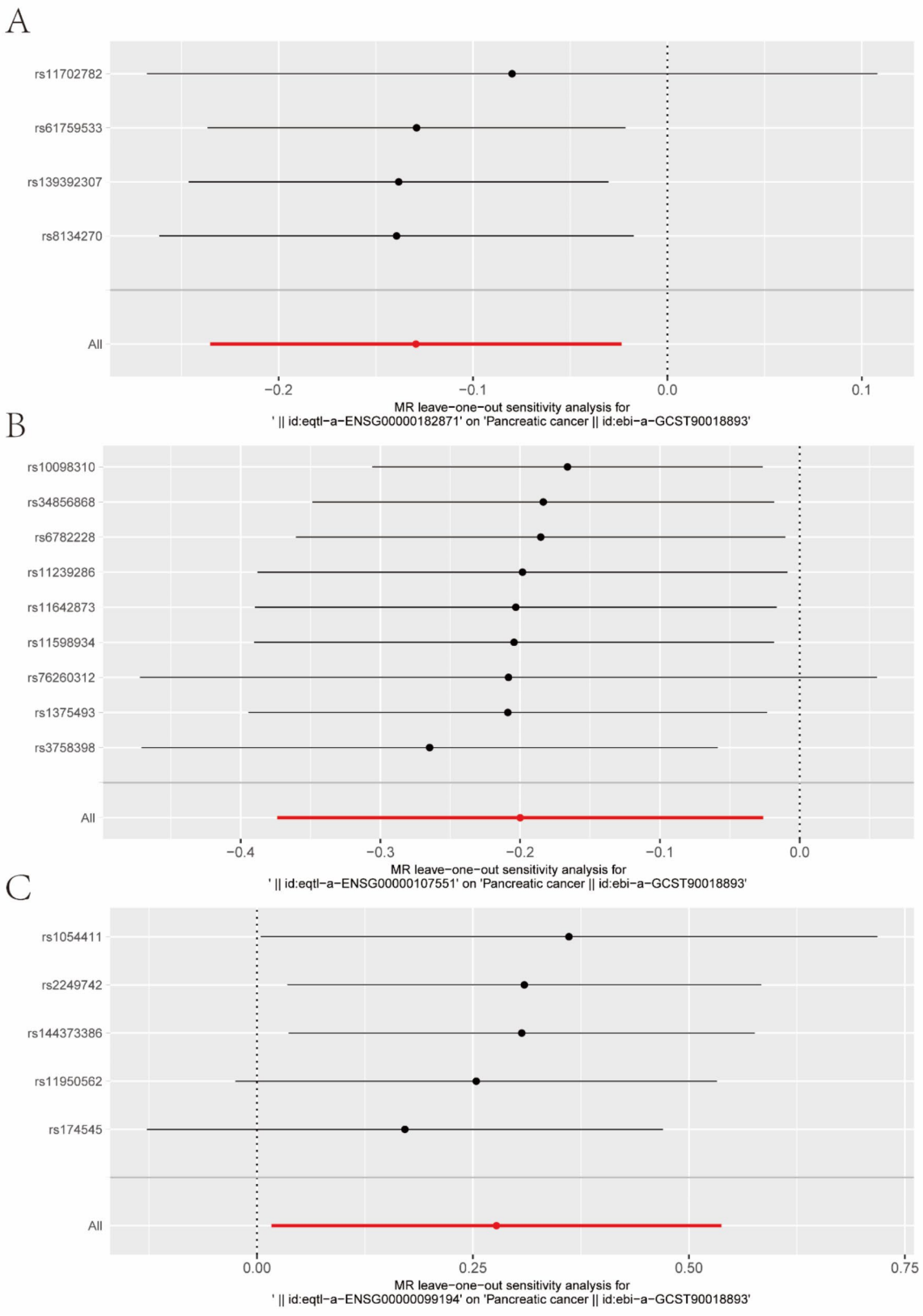

Fig. 4 Leave-out test. (**A**-**C**) Forest plot of Leave-out test for SNPs corresponding to key genes

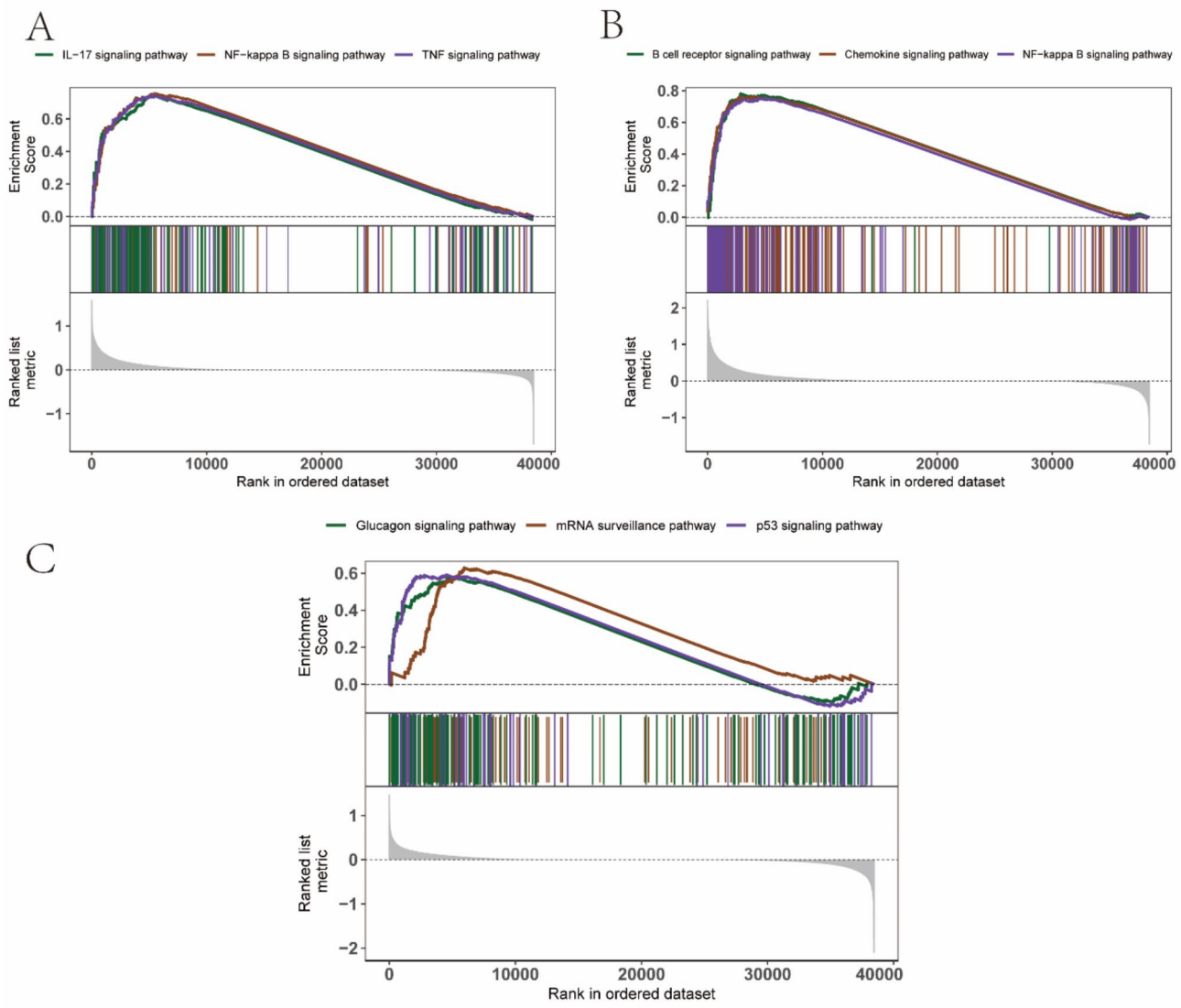

Fig. 5 GSEA analysis of key genes. (**A**) GSEA analysis results of pathways enriched by COL18A1 (IL-17, NF-κB, TNF signaling pathways). (**B**) GSEA analysis results of pathways enriched by RASSF4 (B cell receptor signaling, Chemokine signaling, NF-κB signaling pathways). (**C**) GSEA analysis results of pathways enriched by SCD (Glucagon signaling, mRNA surveillance, p53 signaling pathways)

infiltration [33]. Before infiltrating the peripheral nerves, PDAC cells express a large number of neurotrophic factors, such as nerve sphingomyelin (Artemin), nerve growth factor (NGF), etc., which can produce a strong affinity and sensitivity to the adjacent nerve fiber endings [34]. These neurotrophic factors act as a "glue", causing a phenomenon similar to "mutual attraction" between the two [35]. Prominent perineural alterations were observed during PDAC progression, such as an increase in the size of intrapancreatic nerves (neural hypertrophy), neural density, and neural remodeling [11]. One of the key components of neuropathy is the Schwann cells, the predominant cell type in peripheral nerves [14]. Therefore, in this study, we used a co-culture model of Schwann cells and PDAC cells to mimic the PNI status of PDAC.

During the last decade, many reports have identified the ways in which SCD promotes cancer progression by affecting lipometabolism, cell growth, migration, invasion and metabolism [36], but despite strong preclinical evidence supporting SCD as a therapeutic approach in cancer, the development of highly potent and specific SCD inhibitors has not been a major therapeutic focus, with existing SCD inhibitors having clinical applications limited to the treatment of type 2 diabetes [37]. Here we identify SCD as an important gene present in PDAC neuronal cells that promotes PDAC progression. Further studies designed and tested to knock down SCD with inhibitory effects on PDAC proliferation represent a promising strategy to ameliorate this dilemma of limited therapeutic options.

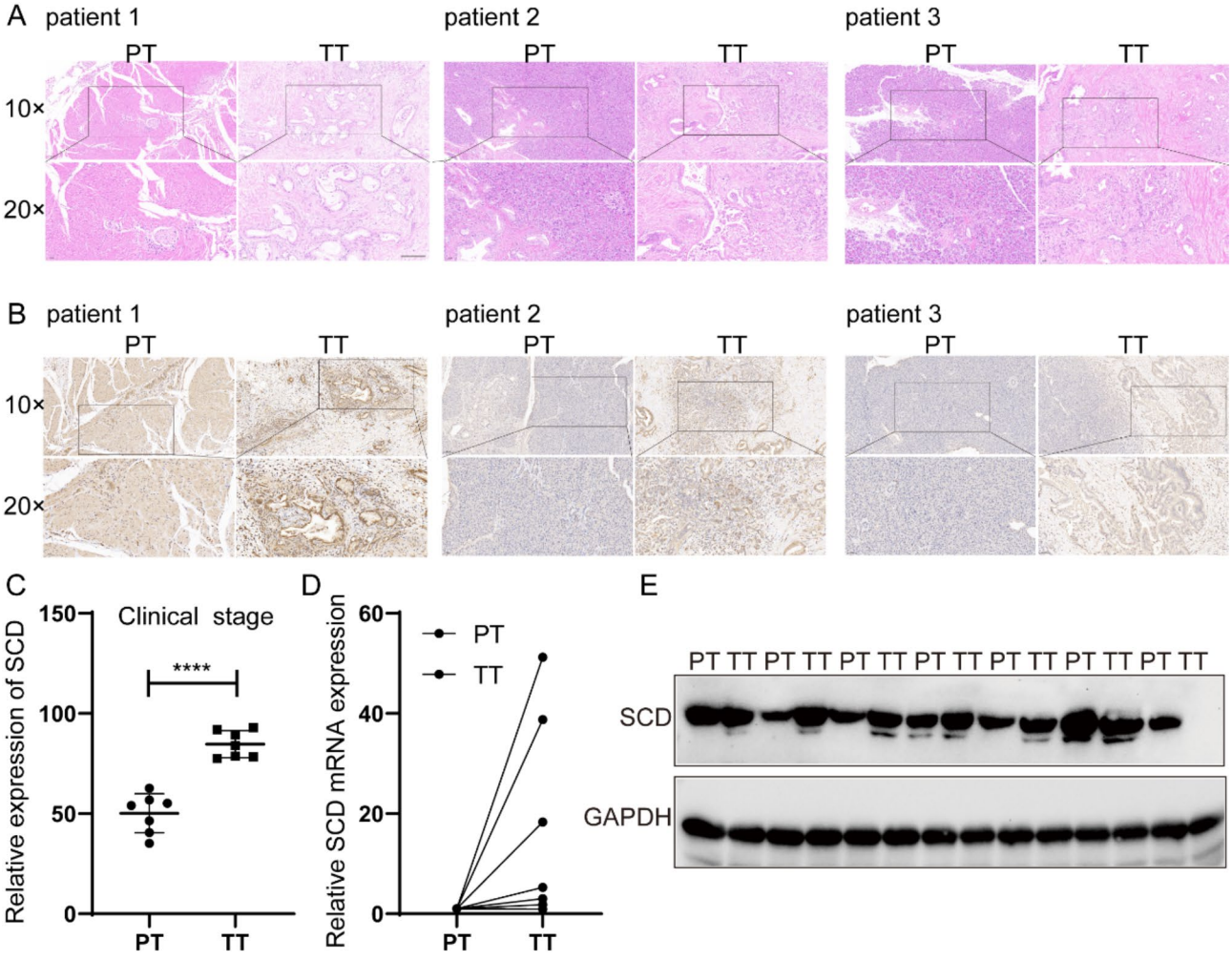

Fig. 6 Expression of SCD in PDAC tissues. (**A**) H&E staining of Rictor in representative xenograft tissue sections, (magnification × 100). Magnified regions are indicated by below line (magnification × 200). (**B**) IHC staining of SCD in representative xenograft tissue sections, (magnification × 100). Magnified regions are indicated by below line (magnification × 200). (**C**) Score according to the degree of cell staining and the proportion of positive cells ($n = 7$) (***$p < 0.001$). (**D**) mRNA expression levels of SCD in TT vs. PT. TT: tumor tissues; PT: paracancerous tissues. (**E**) A representative band image of an immunoblotting assay. GAPDH was employed as a loading control. TT: tumor tissues; PT: paracancerous tissues

This study based on the PDAC single cell database combined with Mendelian randomisation analysis, identified key factors in PDAC neuromarkers associated with PDAC progression, which will contribute to the development of new strategies for neurological treatment of PDAC and the identification of concomitant biomarkers for neurological treatment.

Materials and methods

Data acquisition

1) The database GEO, the full name of GENE EXPRESSION OMNIBUS, is established and maintained by the National Center for Biotechnology Information, NCBI. The single-cell data file of GSE212966 was downloaded from the NCBI GEO open database and contains 10 samples with complete single-cell expression profiles for single-cell analysis. There were 4 control cases and 6 disease cases.

2) The TCGA database is currently the most comprehensive cancer gene information database, containing expression data of genes, miRNA and lncRNA expression data, copy number alterations, DNA methylation, SNP and other information. The original processed expression data of PDAC were downloaded, including normal group ($n = 4$) and tumour group ($n = 179$).

3) Exposed data: The eQTLGen project aims to investigate the genetic structure of gene expression in blood and to better understand the genetic basis of complicated traits. The large-scale eQTLGen project is currently in its second phase and is focused on performing large-scale genome-wide meta-analyzes in blood. eQTL data are generated from the eQTLGen consortium database.

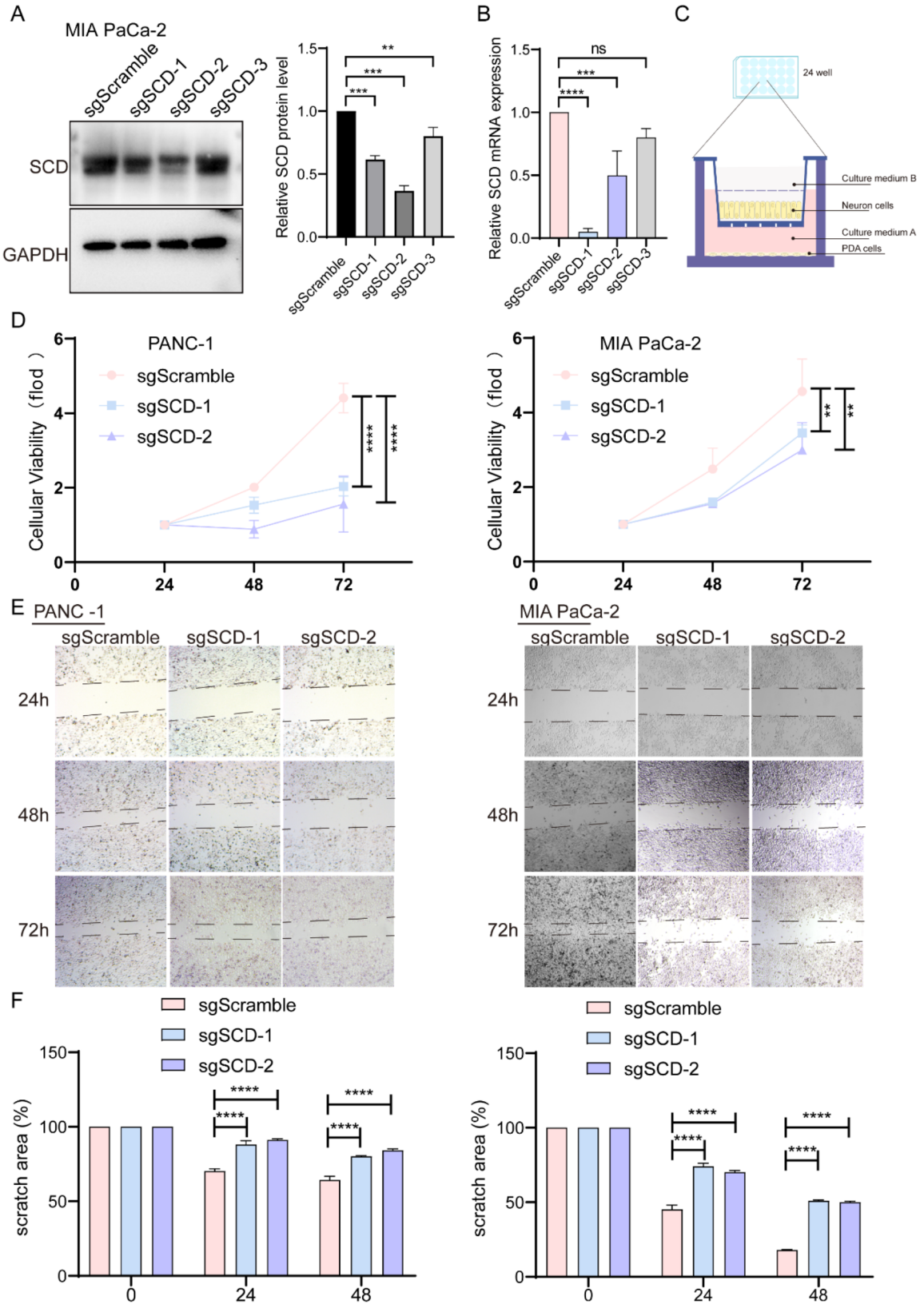

Fig. 7 (See legend on next page.)

(See figure on previous page.)

Fig. 7 The effect of SCD expression on the proliferation and migration ability of PDAC cells. (**A**) The efficacy of the SCD knockdown in Schwann cells was evaluated through IB assays. The knockdown was indicated as sgScramble, sgSCD-1, sgSCD-2 and sgSCD-3. GAPDH was employed as a loading control. (**B**) mRNA expression levels of SCD in sgScramble vs. sgSCD. (**C**) Schematic representation of Schwann Cells and PDAC Cells in co-culture mode. (**D**) Cell viability assay detection of PDAC cells (PANC-1 and MIA PaCa-2) co cultured with SCD knockdown Schwann cells. (**E**) Wound healing assay of PDAC cells co cultured with SCD knockdown Schwann cells. (**F**) The relative percentage of cells exhibiting SCD-induced invasion in PDAC cells (PANC-1 and MIA PaCa-2), ***$p < 0.001$

4) Outcome data: Participants in the outcome-based GWAS studies selected for this review were predominantly of European ancestry. Summary outcome data are all from the EBI database. The GWAS Catalogue now includes publications, top associations and full summary statistics. GWAS Catalogue data are currently mapped to the Genome Assembly and dbSNP Build. There were 1,196 PDAC cases and 475,049 controls.

Quality control

We initially read expression profiles using the Seurat package, where cells were filtered by total number of UMIs per cell, number of expressed genes, percentage of reads for mitochondria per cell, and percentage of reads for ribosomes per cell. Outliers were defined as three MAD from the median. It is generally believed that cells with too high total number of UMI and expressed genes are double cells, and cells with too high mitochondrial reading percentage and ribosome reading percentage are poor quality cells that are on the verge of apoptosis or have become cell debris. After completing the above steps, use DoubletFinder (V2.0.4) to filter the double cells of each sample respectively, thus completing cell quality control.

Data standardization and cell annotation

Use the NormalizeData function to normalize the data, use CellCycleScoring to calculate the cell cycle score, FindVariableFeatures to find hypervariable genes, ScaleData to normalize the data and eliminate the impact of mitochondrial genes, ribosomal genes, and cell cycle on subsequent analysis, and RunPCA to perform expression matrix Perform linear dimensionality reduction, select principal components for subsequent analysis, use Harmony to remove batch effects, it iteratively clusters similar cells in different batches in PCA space while maintaining the diverse batches in each cluster, and use RunUMAP to unify Manifold approximation and projection (UMAP) performs nonlinear dimensionality reduction, FindNeighbors finds neighbor points of cells, and FindClusters divides cells into different cell clusters. By querying CellMarker and PanglaoDB databases and literature, and supplemented by automated annotation with SingleR software, we find the cell types and the respective marker genes present in the corresponding tissue for cell annotation.

Analysis of the interaction between ligand and receptor (Cellchat)

CellChat is a platform that can quantitatively infer and analyze intercellular communication nets from the single-cell data. CellChat analyzes networks and uses pattern recognition methods to predict the major signal in/outputs of cells and how these cells and signals are linked to coordinate function. In our analysis, we used standardised single-cell expression profiles as input data and cell subtypes obtained from single-cell analysis as cell information. We then analyzed the cell-related correlations and used the interaction strengths (weights) between cells and the number of times (counts) to quantify the closeness of the interaction to observe the influence and activity of each cell type in the disease.

Functional analysis of GO and KEGG

In order to comprehensively explore the functional correlations of these important genes, they were functionally annotated using the R package ClusterProfiler. Relevant functional categories were evaluated using Kyoto Encyclopedia of Genes and Genomes (KEGG) and Gene Ontology (GO). KEGG Pathways with both p and q values less than 0.05 were considered to be significant categories.

Mendelian randomization (MR) analysis

Comprehensive summary statistics from hundreds of GWAS studies are available in the EBI database. The EBI database is filtered with the outcome IDs extracted from the GWAS summary data (https://gwas.mrcieu.ac.uk/) and the relevant causal relationships in the eQTL are selected to meet the significance threshold ($P < 1e\text{-}8$), the associated SNPs are selected as potential IVs (instrumental variables), the LD (linkage disequilibrium) between the SNPs is calculated, among the SNPs with $R2 < 0.001$ (clumping window size = 10,000 kb), only $P2 < 5e\text{ -}8$ SNPs are retained. (The weighted median approach allows correct causal estimation up to 50% of the time when the IV is null), MR-Egger (the weighted model estimate is more capable of detecting causal effects, less biased, and with a lower type I error rate than the MR-Egger regression). A statistical method to assess the reliability of causality to provide an overall estimate of the effect of all cis and some cross-regional gene expression in whole blood on PDAC (if there is only one statistical method for the SNP in the causal relationship, only the Wald ratio is used).

Sensitivity analysis

To assess the impact of specific genetic variants on PDAC risk, we used Mendelian randomisation (MR) leave-one-out sensitivity analysis. This method systematically excludes each SNP and recalculates the pooled effect size of the remaining SNPs to identify and remove variants that disproportionately affect the overall estimate. Removing each SNP produces a new point estimate and its 95% confidence interval to help assess the unique contribution and robustness of the SNP to the overall results. This graph summarises the estimates after removing individual SNPs, as well as the overall estimate when all SNPs are included. To determine the robustness of our analysis, by comparing these estimates we can observe the effect of removing a single SNP on the overall results.

GSEA pathway enrichment analysis

The differences in signalling pathways between the high and low expression groups were further analyzed using GSEA [38]. The background gene set is the annotated gene set of version 7.0, which was downloaded from the MsigDB database. As the annotated gene set for subtype pathways, we performed differential expression analysis of pathways among subtypes and analyzed significantly enriched gene sets based on the consistency score (adjusted p-value less than 0.05) for sorting. GSEA analysis is often used in studies where disease classification and biological significance are closely linked.

Clinical specimen collection

The clinical samples used in this study were collected from PDAC patients undergoing pancreatic surgery in the Liaoning Cancer Hospital. Patients were all confirmed pathologically and diagnosed with PDAC. Cancer and matched paracancer tissue were snap frozen in liquid nitrogen immediately after resection and then stored at -80 °C prior to use. This trial was authorized by the Ethics Committee of Liaoning Cancer Hospital and conducted in accordance with the Declaration of Helsinki.

Histology & IHC

The tissue processing of FFPE organotypic matrices and tumor tissues was performed on a Leica Peloris using standard tissue processing protocols. FFPE samples were sectioned at 4 μm (Leica RM2235 microtome). Sections were placed on a plain glass slide for H&E staining or a positively charged slide for IHC. Sections were deparaffinised and stained with haematoxylin, Australian biostain and eosin using standard H&E procedures on a Leica ST5010 Autostainer XL.

Detect mRNA expression using qRT-PCR

PCR reaction was performed with 100 ng of cDNA on a Rotor-Gene®-Q real-time PCR cycler (Roche LightCycler 96) using TaqMan Universal PCR Master Mix (Applied Biosystems). Recycling conditions were: 10 min denaturation at 95℃ and 40 cycles at 95℃ for 15 s and at 60℃ for 1 min. The expression levels were normalised to the expression of GAPDH, which was used as an internal control. The primer sequences for use in qRT-PCR are shown below:

SCD	**5′-GCACATCAACTTCACCACATTCTTC-3′**
SCD	3′-CAGCCACTCTTGTAGTTTCCATCTC-5′
GAPDH	5′-TGTGGGCATCAATGGATTTGG-3′
GAPDH	3′-ACACCATGTATTCCGGGTCAAT-5′

Immunoblotting assay

Total proteins were extracted using RIPA whole cell lysis solution. Proteins were separated by 10% SDS-PAGE electrophoresis, measured and transferred to PVDF membranes (Millipore, Billerica, MA, USA) in a semi-dry state. Membranes were blocked with TBS + Tween (TBST) containing 5% skim milk powder for 1 h, washed and incubated with primary antibody (ABclonal, A16429, 1:1000) overnight at 4℃. The membranes were then washed and exposed to a horseradish peroxidase-labelled secondary antibody for 1 h. After washing the membrane, the chemiluminescent substrate was applied and the grey scale values were measured using a gel imaging system.

Cell culture and transfection

The human Schwann cell line, the human PDAC cell lines PANC-1 (CRL-1469) and MIA PaCa-2 (CRL-1420) were obtained from the ATCC. All cell lines were grown at 37℃ in a humidified incubator containing 5% CO_2. In vitro growing cell lines were treated with small guide RNA (sgRNA) against SCD (ABM, China) genes and sgScramble (ABM, China). After Schwann cells were fully attached, sg-RNA was transfected at a final concentration of 100 nM and incubated 48 h. The sgRNA sequences are listed below:

Name	**Target**	**Sequence**
sgSCD-1	1–11	5′-CACATCGTCCTGCAGCAAGT-3′
sgSCD-2	2-118	5′-ATGTCGTCTTCCAAGTAGAG-3′
sgSCD-3	3-159	5′-TATATATGACCCCACCTACA-3′

Co-culture of Schwann and PDAC cells in vitro

For Transwell-based co-cultures, 2×10^5 PDAC cells were seeded in the lower section of six-well plates with 2×10^5 Schwann cells seeded on top of the Transwell membrane (0.4 μm, Corning). Following 48 h of co-culture, the PDAC cells were washed three times with PBS, and then an equal number of the PDAC cells were cultured individually in fresh medium for 24–48 h, and then the cells were harvested for further study.

Wound healing migration assay

After cultivating PDAC cells individually for 24–48 h in a 6-well plate, the cells were scratched with a 200-μL tip and the lines, both horizontal and vertical, were scratched three times per well. Ensure that the force is uniform and that the tip is perpendicular. Wash the cells with pre-warmed PBS, add 2 mL fresh medium (0–3% FBS) to each well and continue incubation. Photographs of the scratches were taken at 0 and 48 h. Image J was then used to measure the area of the cell scratches and the wound healing rate was used to reflect the ability of the cells to migrate.

Cell proliferation assay

After PDAC cells were cultured alone for 24 h, cells were transfected into 96-well plates at a density of 2×10^3 cells/well. From day 1 to day 3, the serum-free medium containing 10% CCK-8 (APExBIO, USA) reagent solution was added to replace the primary medium and incubated for 1 h. Light absorption was measured at 450 nm (OD-450).

Statistical analysis of data

A reliable MR analysis is relied on three assumptions: [1] correlation assumption (instrumental variables are strongly related to exposure but not to outcomes directly) [2], independence assumption (instrumental variables are unrelated to confounding factors) [3], Exclusivity hypothesis (instrumental variables can affect outcomes only through exposure. If the IV can affect outcomes through other pathways, then gene pleiotropy is established). The R language (version 4.3.0) was used in this analysis.

All data in this experiment were generated using GraphPad Prism 7 software. A two-tailed t-test or one-way ANOVA was used to analyze the data differences. The results were shown as mean ± standard error. Significant difference: $^{*}p < 0.05$, $^{**}p < 0.01$, $^{***}p < 0.001$.

Conclusion

PDAC peripheral nerve cells are able to influencing the development of PDAC, and the high expression of SCD in nerve cells has a promoting effect on the development of PDAC.

Abbreviations

ATCC	American Type Culture Collection
BDNF	Brain-derived neurotrophic factor
FFPE	Formalin fixation and paraffin embedding
GO	Gene Ontology
GWAS	Genome-wide association analyzes
IHC	Immunohistochemical, Instrumental variables
IVs	Linkage disequilibrium
KEGG	Kyoto Encyclopedia of Genes and Genomes
LD	MR, Mendelian Randomization
MAD	Median absolute deviations
MIR	M/I ratio
NGF	Nerve growth factor
NGF	Nerve growth factor
PDAC	Pancreatic ductal adenocarcinoma
PanIN	Pancreatic intraepithelial neoplasia
PNI	Perineural invasion
q-RTpcr	Real-time fluorescence quantitative PCR
SCD	Stearoyl Coenzyme A Desaturase
UMAP	Unify Manifold approximation and projection

Supplementary Information

The online version contains supplementary material available at https://doi.org/10.1186/s12935-025-03682-5.

Supplementary Material 1

Supplementary Material 2

Supplementary Material 3

Acknowledgements

We thank the Science and Technology Program of Liaoning Province (2023021040-JH2/1017) and Liaoning Provincial Key Laboratory of Precision Medicine for Malignant Tumors (Project number: 220569).

Author contributions

Xue Zhang and Ling-Xiao Zhao wrote the manuscript, Si-Qi Cheng revised the manuscript. Ye-Fu Liu approved and revised the final manuscript. All authors have read and approved the final manuscript.

Funding

This study was financially supported by the Science and Technology Program of Liaoning Province (2024-BS-322) and the Liaoning Provincial Key Laboratory of Precision Medicine for Malignant Tumors (Project number: 220569).

Data availability

No datasets were generated or analysed during the current study.

Declarations

Ethics approval and consent to participate

The study was conducted in accordance with the Declaration of Helsinki and was approved by the Ethics Committee of Liaoning Cancer Hospital (Approval Number: KY20240501).

Consent for publication

All participants gave written informed consent prior to participation. Personal information was anonymized and deidentified to protect participant privacy. Our study was completed in accordance with the Declaration of Helsinki. All experiments were performed in accordance with relevant guidelines and regulations. The datasets generated during the current study are available from the corresponding author on reasonable request.

Competing interests

The authors declare no competing interests.

Author details

[1]Central Laboratory, Cancer Hospital of Dalian University of Technology, Liaoning Cancer Hospital & Institute, Shenyang, Liaoning 110042, China
[2]Key Laboratory of Medical Cell Biology of Ministry of Education, Key Laboratory of Major Chronic Diseases of Nervous System of Liaoning Province, Health Sciences Institute of China Medical University, Shenyang 110122, China
[3]China Medical University, Shenyang, Liaoning 110122, China
[4]Department of Hepatobiliary and Pancreatic Surgery, Cancer Hospital of Dalian University of Technology, Liaoning Cancer Hospital & Institute, No. 44 Xiaoheyan Road, Dadong District, Shenyang, Liaoning 110042, China

Received: 9 September 2024 / Accepted: 7 February 2025
Published online: 20 February 2025

References

1. Hezel AF, Kimmelman AC, Stanger BZ, Bardeesy N, Depinho RA. Genetics and biology of pancreatic ductal adenocarcinoma. Genes Dev. 2006;20(10):1218–49.
2. Fuchs CS, Colditz GA, Stampfer MJ, Giovannucci EL, Hunter DJ, Rimm EB, et al. A prospective study of cigarette smoking and the risk of pancreatic cancer. Arch Intern Med. 1996;156(19):2255–60.
3. Gapstur SM, Gann PH, Lowe W, Liu K, Colangelo L, Dyer A. Abnormal glucose metabolism and pancreatic cancer mortality. JAMA. 2000;283(19):2552–8.
4. Schenk M, Schwartz AG, O'Neal E, Kinnard M, Greenson JK, Fryzek JP, et al. Familial risk of pancreatic cancer. J Natl Cancer Inst. 2001;93(8):640–4.
5. Bartsch DK. Familial pancreatic cancer. Br J Surg. 2003;90(4):386–7.
6. Whitcomb DC, Gorry MC, Preston RA, Furey W, Sossenheimer MJ, Ulrich CD, et al. Hereditary pancreatitis is caused by a mutation in the cationic trypsinogen gene. Nat Genet. 1996;14(2):141–5.
7. Jaffee EM, Hruban RH, Canto M, Kern SE. Focus on pancreas cancer. Cancer Cell. 2002;2(1):25–8.
8. Thompson D, Easton DF, Breast Cancer Linkage C. Cancer incidence in BRCA1 mutation carriers. J Natl Cancer Inst. 2002;94(18):1358–65.
9. Bray F, Laversanne M, Sung H, Ferlay J, Siegel RL, Soerjomataram I, et al. Global cancer statistics 2022: GLOBOCAN estimates of incidence and mortality worldwide for 36 cancers in 185 countries. CA Cancer J Clin. 2024;74(3):229–63.
10. Siegel RL, Miller KD, Wagle NS, Jemal A. Cancer statistics, 2023. CA Cancer J Clin. 2023;73(1):17–48.
11. Demir IE, Friess H, Ceyhan GO. Neural plasticity in pancreatitis and pancreatic cancer. Nat Rev Gastroenterol Hepatol. 2015;12(11):649–59.
12. Renz BW, Takahashi R, Tanaka T, Macchini M, Hayakawa Y, Dantes Z, et al. beta2 adrenergic-neurotrophin Feedforward Loop promotes pancreatic Cancer. Cancer Cell. 2018;33(1):75–90. e7.
13. Renz BW, Takahashi R, Tanaka T, Macchini M, Hayakawa Y, Dantes Z, et al. beta2 adrenergic-neurotrophin Feedforward Loop promotes pancreatic Cancer. Cancer Cell. 2018;34(5):863–7.
14. Xue M, Zhu Y, Jiang Y, Han L, Shi M, Su R, et al. Schwann cells regulate tumor cells and cancer-associated fibroblasts in the pancreatic ductal adenocarcinoma microenvironment. Nat Commun. 2023;14(1):4600.
15. Demir IE, Boldis A, Pfitzinger PL, Teller S, Brunner E, Klose N et al. Investigation of Schwann cells at neoplastic cell sites before the onset of cancer invasion. J Natl Cancer Inst. 2014;106(8).
16. Hogeweg P. The roots of bioinformatics in theoretical biology. PLoS Comput Biol. 2011;7(3):e1002021.
17. Sekula P, Del Greco MF, Pattaro C, Kottgen A. Mendelian randomization as an Approach to assess causality using Observational Data. J Am Soc Nephrol. 2016;27(11):3253–65.
18. Larsson SC, Butterworth AS, Burgess S. Mendelian randomization for cardiovascular diseases: principles and applications. Eur Heart J. 2023;44(47):4913–24.
19. Wang H, Guo M, Wei H, Chen Y. Targeting p53 pathways: mechanisms, structures, and advances in therapy. Signal Transduct Target Ther. 2023;8(1):92.
20. Carioli G, Bertuccio P, Levi F, Boffetta P, Negri E, La Vecchia C et al. Cohort analysis of Epithelial Cancer Mortality Male-to-female sex ratios in the European Union, USA, and Japan. Int J Environ Res Public Health. 2020;17(15).
21. Tesfay L, Paul BT, Konstorum A, Deng Z, Cox AO, Lee J, et al. Stearoyl-CoA desaturase 1 protects ovarian Cancer cells from ferroptotic cell death. Cancer Res. 2019;79(20):5355–66.
22. Dobrzyn P, Bednarski T, Dobrzyn A. Metabolic reprogramming of the heart through stearoyl-CoA desaturase. Prog Lipid Res. 2015;57:1–12.
23. Scaglia N, Igal RA. Stearoyl-CoA desaturase is involved in the control of proliferation, anchorage-independent growth, and survival in human transformed cells. J Biol Chem. 2005;280(27):25339–49.
24. Mason P, Liang B, Li L, Fremgen T, Murphy E, Quinn A, et al. SCD1 inhibition causes cancer cell death by depleting mono-unsaturated fatty acids. PLoS ONE. 2012;7(3):e33823.
25. Roongta UV, Pabalan JG, Wang X, Ryseck RP, Fargnoli J, Henley BJ, et al. Cancer cell dependence on unsaturated fatty acids implicates stearoyl-CoA desaturase as a target for cancer therapy. Mol Cancer Res. 2011;9(11):1551–61.
26. Sen U, Coleman C, Sen T. Stearoyl coenzyme a desaturase-1: multitasker in cancer, metabolism, and ferroptosis. Trends Cancer. 2023;9(6):480–9.
27. Benam KH, Villenave R, Lucchesi C, Varone A, Hubeau C, Lee HH, et al. Small airway-on-a-chip enables analysis of human lung inflammation and drug responses in vitro. Nat Methods. 2016;13(2):151–7.
28. Han JH, Lee HW, Jung SH, Cho CW, Kim TJ, Kang JS, et al. The anti-obesity effect of mulberry leaf (Mori Folium) extracts was increased by bioconversion with Pectinex. Sci Rep. 2022;12(1):20375.
29. Southam AD, Khanim FL, Hayden RE, Constantinou JK, Koczula KM, Michell RH, et al. Drug redeployment to kill leukemia and lymphoma cells by disrupting SCD1-Mediated synthesis of Monounsaturated fatty acids. Cancer Res. 2015;75(12):2530–40.
30. Liu Q, Ma Z, Cao Q, Zhao H, Guo Y, Liu T, et al. Perineural invasion-associated biomarkers for tumor development. Biomed Pharmacother. 2022;155:113691.
31. Nomura A, Majumder K, Giri B, Dauer P, Dudeja V, Roy S, et al. Inhibition of NF-kappa B pathway leads to deregulation of epithelial-mesenchymal transition and neural invasion in pancreatic cancer. Lab Invest. 2016;96(12):1268–78.
32. Li J, Kang R, Tang D. Cellular and molecular mechanisms of perineural invasion of pancreatic ductal adenocarcinoma. Cancer Commun (Lond). 2021;41(8):642–60.
33. Na'ara S, Gil Z, Amit M. In Vitro modeling of cancerous neural Invasion: the dorsal Root Ganglion Model. J Vis Exp. 2016(110):e52990.
34. Demir IE, Schafer KH, Tieftrunk E, Friess H, Ceyhan GO. Neural plasticity in the gastrointestinal tract: chronic inflammation, neurotrophic signals, and hypersensitivity. Acta Neuropathol. 2013;125(4):491–509.
35. Jobling P, Pundavela J, Oliveira SM, Roselli S, Walker MM, Hondermarck H. Nerve-Cancer cell cross-talk: a novel promoter of Tumor Progression. Cancer Res. 2015;75(9):1777–81.
36. Tracz-Gaszewska Z, Dobrzyn P. Stearoyl-CoA desaturase 1 as a therapeutic target for the treatment of Cancer. Cancers (Basel). 2019;11(7).
37. Zhang Z, Dales NA, Winther MD. Opportunities and challenges in developing stearoyl-coenzyme A desaturase-1 inhibitors as novel therapeutics for human disease. J Med Chem. 2014;57(12):5039–56.
38. Subramanian A, Tamayo P, Mootha VK, Mukherjee S, Ebert BL, Gillette MA, et al. Gene set enrichment analysis: a knowledge-based approach for interpreting genome-wide expression profiles. Proc Natl Acad Sci U S A. 2005;102(43):15545–50.

Publisher's note